Vietnam Journal of Earth Sciences, 44(1), 127-143, https://doi.org/10.15625/2615-9783/16974

Vietnam Academy of Science and Technology
Vietnam Journal of Earth Sciences
http://www.vjs.ac.vn/index.php/jse

Projected future changes in drought characteristics over Southeast Asia

Phuong Nguyen-Ngoc-Bich[1], Tan Phan-Van[1], Long Trinh-Tuan[2], Fredolin T. Tangang[3], Faye Cruz[4], Jerasorn Santisirisomboon[5], Liew Juneng[3], Jing Xiang Chung[6], Edvin Aldrian[7]

[1]*Hydrology and Oceanography, VNU University of Science, Vietnam National University, Hanoi, Vietnam*
[2]*Center for Environmental Fluid Dynamics, VNU University of Science, Hanoi, Vietnam*
[3]*Faculty of Science and Technology, Universiti Kebangsaan Malaysia, Bangi, Malaysia*
[4]*Regional Climate Systems Laboratory, Manila Observatory, Quezon City, Philippines*
[5]*Ramkhamhaeng University Center of Regional Climate Change and Renewable Energy (RU-CORE), Ramkhamhaeng University, Bangkok, Thailand*
[6]*Faculty of Science and Marine Environment, Universiti Malaysia Terengganu, Kuala Nerus, Terengganu, Malaysia*
[7]*Agency for the Assessment and Application of Technology, Agency for the Assessment and Application of Technology (BPPT), Jakarta*

Received 06 October 2021; Received in revised form 07 February 2022; Accepted 07 March 2022

ABSTRACT

This study analyzes projected changes in drought characteristics over Southeast Asia for the mid and late 21st century under Representative Concentration Pathway (RCP) scenarios (RCP4.5 and RCP8.5) that participated in IPCC AR5. Drought characteristics are computed using the standardised precipitation index (SPI) with 12-month time scales based on precipitation data from the multi-model downscaled experiments of the Coordinated Regional Climate Downscaling Experiment-Southeast Asia (CORDEX-SEA). Comparison with observations indicates that model uncertainties are high over Myanmar, southern China, and some areas of the Maritime Continent. The multi-model ensemble is in best agreement with the observation relative to individual models. Under the future projections, the ensemble model exhibits no significant changes in duration and severity of drought for all scenarios in the mid 21st century. However, the drought characteristics are projected to become shorter and more severe for RCP8.5 in the late 21st century. Projected changes in inter-arrival time, maximum intensity, frequency, and geographic extent also indicate more frequent and severe drought over the mainland in the late 21st century for RCP8.5.

Keywords: Drought, SPI, regional climate, Southeast Asia, CORDEX-SEA.

1. Introduction

Global warming is likely to be associated with changes in the hydrological cycle and extreme events such as droughts. Dai (2013) suggested severe and widespread droughts in the 21st century over many land areas connected with either decrease in precipitation and/or increase in evapotranspiration. Touma et al. (2015) and Spinoni et al. (2020) showed that droughts likely become more frequent

*Corresponding author, Email: phuongnnb@hus.edu.vn

and severe over southern South America, the Mediterranean region, southern Africa, southeastern China, Japan, and southern Australia. The increasing trends of drought were found in Europe (Spinoni et al., 2018; Lehner et al., 2017), North America (Cook et al., 2010; Swain and Hayhoe, 2015), Africa (Abiodun et al. 2019), East Asia (Zhang and Zhou, 2015; Kim et al., 2021), and West Asia (Kim and Byun, 2009). In contrast, decreasing drought trends were detected in East Asia (Burke et al., 2006; Dai, 2013; Zhang and Zhou, 2015; Kim et al., 2021) and most parts of China (Huo-Po et al., 2013). Southeast Asia is a region that has a high risk of drought in the future. Drought is likely to increase in the lower Mekong River basin over the 21st century (Thilakarathne and Sridhar, 2017). Tangang et al. (2020) illustrated that dry conditions would likely prevail over the Maritime Continent, particularly over the Indonesian region.

Global climate models (GCMs) are a fundamental research tool for understanding climate and are widely used to examine future drought conditions (e.g., Seager et al., 2007; Prudhomme et al., 2014; Cook et al., 2020). Besides, regional climate models (RCMs) allow us to describe precisely small-scale processes and features. RCMs have recently become popular for examining drought conditions on regional and local scales (Rummukainen, 2010; Spinoni et al., 2020). To examine drought conditions, studies may need to consider the models' internal and external factors that influence the reliability of simulations. For example, Dai (2013) found that the differences between observed and simulated droughts are mainly due to natural variations in tropical sea surface temperatures. Rhee and Cho (2016) demonstrated that the changes in drought frequency largely depend on the choices of drought indices rather than climate projection scenarios. Zhao and Dai (2017) and Zhai et al. (2020) described the importance of evapotranspiration and the choice of evapotranspiration schemes for projected drought.

Southeast Asia has experienced moderate to severe droughts in the past (Le et al., 2019; ESCAP, 2020). For example, the decreasing duration of precipitation due to changes in monsoon activity results in drought in this region (Endo et al., 2009; Deni et al., 2010). The causes of drought in Southeast Asia are inherently complex, leading to a significant difference of drought conditions from year to year. Droughts are affected by various climatic factors, mainly the El Niño-South Oscillation (ENSO) and the Indian Ocean Dipole (IOD) (Cai et al., 2013; Tangang et al., 2017). As evapotranspiration is likely to increase due to climate change, the risk of drought is potentially increasing across the region (Tangang et al., 2020a).

The objective of this study is to investigate projected changes in drought characteristics over SEA. Drought characteristics are computed based on the standardized precipitation index with 12-month time scales (SPI-12; McKee et al., 1993), which is widely used in predicting and monitoring drought events (Jamshidi et al., 2011; Bayissa et al., 2018). As input data, we use RCM employed by the Coordinated Regional Climate Downscaling Experiment Southeast Asia (CORDEX-SEA; Giorgi et al., 2009; Juneng et al., 2016; Ngo-Duc et al., 2017) with 0.25° horizontal resolution under RCP4.5 and RCP8.5 scenarios (van Vuuren, 2011). In the following, the data and methods are described in Section 2. Section 3 presents the validation of simulated drought and the assessment of projected changes in drought characteristics over SEA for the mid and late 21st century under RCP4.5 and RCP8.5. Section 4 discusses and summarizes the findings of the study.

2. Data and methods

2.1. Study area

The study has been carried out for the Southeast Asia Regional Climate

Downscaling (SEACLID)/CORDEX-SEA domain of 15°S to 27°N, 89°E to 146.5°E (Fig. 1). This region is geographically situated east of the Indian subcontinent, south of China, and northwest of Australia. The region is located between the Indian Ocean and the Bay of Bengal in the west, the Philippine Sea, the East Sea, and the Pacific Ocean in the east. There are two sub-regions within the study domain. The first sub-region is Mainland Southeast Asia (referred to as the mainland), also known as the Indochinese Peninsula, comprises Cambodia, Laos, Myanmar, Peninsular Malaysia, Thailand, and Vietnam. The second sub-region is Maritime Southeast Asia (referred to as the "Maritime Continent"), also known as the Malay Archipelago, comprises Brunei, the Australian Islands, East Malaysia, East Timor, Indonesia, the Philippines, and Singapore.

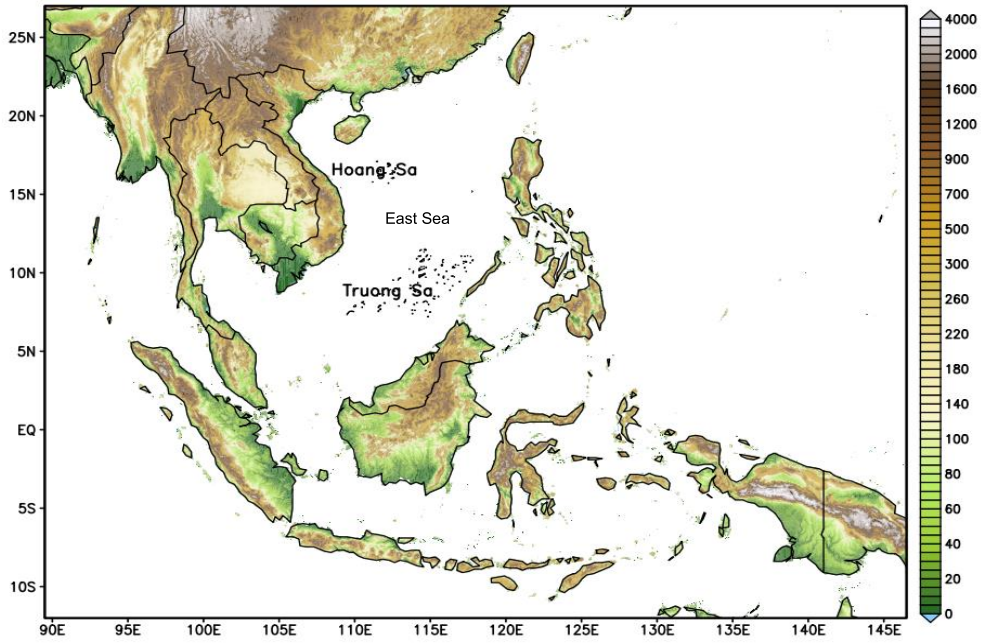

Figure 1. CORDEX-SEA domain

2.2. Data

The Asian Precipitation-Highly Resolved Observational Data Integration Towards Evaluation of the Water Resources (APHRODITE) data (Yatagai et al., 2012) is used for validating climate inputs and estimating drought characteristics. The APHRODITE data has a resolution of 0.25° × 0.25° and covers the period 1976-2005 on a daily time scale over the Asian monsoon region, including SEA. The dataset was created based on gauged-based rainfall (approximately 12,000 rain gauge stations across the entire Asian region), and the angular distance weighting interpolation method was used to grid rainfall observations (Yatagaiet et al., 2012; Sushama et al., 2014). The APHRODITE data was also corrected using satellite-based rainfall (Yatagai et al., 2012).

The Regional Climate Model (RegCM) downscaled the outputs of six Coupled Model Intercomparison Project Phase 5 (CMIP5) Global Climate Models (GCMs) to assess potential future changes in drought characteristics for Vietnam within the framework of the CORDEX-SEA project. The list of the GCMs as well as the names of the RegCM outputs can be found in Table 1 of

Nguyen-Ngoc-Bich et al. (2021). Both GCMs and RegCMs were continuously integrated until the end of the 21st century (2100), including a baseline period (1976-2005), and for two RCP4.5 and RCP8.5 scenarios. The RegCM used here is a hydrostatic, limited area model with a sigma (σ) vertical coordinate (Giorgi et al., 2012). The model was set up similarly to (Ngo-Duc et al., 2017; Juneng et al., 2016), with the Biosphere-Atmosphere Transfer Scheme (Giorgi et al., 1993), the Community Climate Model version 3 radiation scheme (Giorgi et al., 1999), and the MIT-Emanuel convective and ocean flux schemes (Emanuel and Zivkovic-Rothman, 1999). For the CORDEX-SEA model domain of 15°S to 27°N, 89°E to 146.5°E (Fig. 1), the model was run with 18 vertical levels and 25 km of horizontal resolution (Tangang et al. 2020). Future greenhouse gas scenarios RCP4.5 and RCP8.5 were chosen as the lower and higher emission scenarios, respectively.

All 6-hourly precipitation data from the six RegCM simulations and their ensemble mean were aggregated to monthly values before being extracted into three periods: the baseline period (1976-2005), the middle of the 21st century period (MF, 2036-2065), and the end of the 21st century period (FF, 2071-2100).

Table 1. List of selected downscaled experiments with their respective driving CMIP5 GCMs used in this study

No.	Abbreviation of the RCM experiment	Driving GCM	Country and Institution that developed the GCM	Horizontal Resolution (degrees)
1	CNRM	CNRM-CM5	Centre national de Recherches Meteorologiques, France	1.41 × 1.41
2	HadG	HadGEM2	Hadley Centre, United Kingdom	1.25 × 1.875
3	MPI	MPI-ESM-MR	Max Planck Institue for Meteorology, Germany	1.875 × 1.875
4	ECEA	EC-Earth	EC-Earth consortium, European Union	1.125 × 1.125
5	CSIR	CSIRO	Commonwealth Scientific and Industrial Research Organisation, Australia	1.875 × 1.875
6	GFDL	GFDL-ESM2M	Geophysical Fluid Dynamics Laboratory, United States	2.5 × 2.0
7	ENS	Ensemble mean of all six downscaled experiments		

2.3. The Standardized Precipitation Index and drought characteristics

McKee et al. (1993) generated the Standardized Precipitation Index (SPI) to identify and monitor drought events based on monthly rainfall data for the desired time period in a particular location. The available long-term rainfall data is fitted to the gamma probability distribution, which is then transformed to a normal distribution, to ensure a mean of zero for SPI time series for the location and desired period (Svoboda et al., 2012). It is designed to identify drought periods as well as the severity of droughts at various time intervals, such as 1, 3, 6, 9, 12, or 24 months. However, the appropriate time step may be determined by the purpose of the drought analysis. Positive SPI values indicate more precipitation than average, while negative values indicate less precipitation than average. Both dry and wet conditions can be monitored using the SPI. A drought event begins when the SPI value reaches -1.0 and ends when the SPI value returns to positive. The complete procedure for estimation of SPI is available in Edwards and Mckee (1997). In this study, we use the SPI index for the 12-month timescale (referred to as SPI-12), which reflects the impact of drought on the availability of water resources related to long-term precipitation anomalies. The timescale of SPI is suitable for examining long-term meteorological droughts.

A drought spell (or a drought event) is defined as a period of dryness with the SPI-12 values below a truncation value. The

truncation level for the droughts is selected as -1; this allows capturing droughts that are moderate to extreme drought conditions (McKee et al., 1993). Drought characteristics are listed below and shown in Fig. 2:

(a) Drought duration (DD): DD of an event is the number of consecutive months in which the SPI-12 is less than -1;

(b) Drought severity (DS): DS of an event is the absolute value of the sum of the SPI-12 values for each month in which the drought event occurs;

(c) Inter-arrival time of drought (ITD, Cancelliere et al., 2003; Mishra et al., 2009): It is the number of months between starting months of two consecutive drought events;

(d) Maximum intensity of drought (max ID): max ID of an event is defined as the absolute value of the minimum SPI of a drought event.

In this study, we have calculated the means of DD, DS, ITD and max ID for a specific period (BL, MF, FF period):

$$\overline{CHAR} = \frac{1}{N}\sum_{i=1}^{N} CHAR_i \quad (1)$$

where $\overline{CHAR}$ is the mean of a drought characteristic (i.e., DD, DS, ITD, and max ID) for a period. $CHAR_i$ is the drought characteristic for an i^{th} event in the period. N is the number of drought events that occurred in the period.

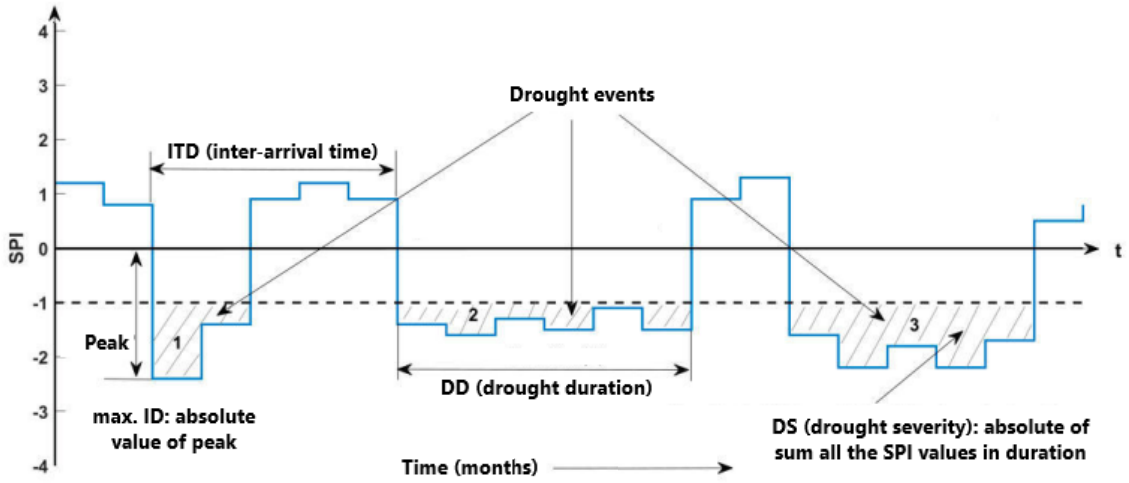

Figure 2. Sketch of drought characteristics using the SPI

In addition, we evaluate the drought frequency (DF) for years. DF of a year is the number of drought events that occurred in the year. Mean DF of the domain is computed for each year. Furthermore, we assess drought spatial geographic extent (SE, Brunner et al., 2021) on a monthly scale. Monthly SE is the percentage of grid points where drought occurs in a given month. Monthly mean SE of a period is calculated for all months.

2.4. Assessment methods

The differences (Δ_b) between model simulations (M_b) and observation (O_b, APHRODITE data) for the baseline are calculated to validate the model performance of annual precipitation and drought characteristics. The differences in annual precipitation, drought severity, inter-arrival time, maximum intensity and geographic extent are calculated following the equation:

$$\Delta_b = \frac{(M_b - O_b)}{O_b} \times 100\% \quad (2)$$

The differences in drought duration and drought frequency are calculated following the equation:

$$\Delta_b = M_b - O_b \quad (3)$$

in which, M_b is the average magnitude of the model variable and O_b is the average magnitude of the observed variable for the baseline period.

The projected changes (Δ_f) in annual precipitation and average drought characteristics are identified by the changes between the model variable in the future periods (M_f) and this model variable in the baseline (M_b). If we assume that the errors in the simulations are mainly systematic, then the difference will cancel out the systematic errors and result in changes of variables between different periods due to climate fluctuations and boundary conditions. The projected changes of annual precipitation, drought severity, inter-arrival time, maximum intensity, and geographic extent are calculated following the equation:

$$\Delta_f = \frac{M_f - M_b}{M_b} \times 100\% \quad (4)$$

The projected changes of drought duration and drought frequency are calculated following the equation:

$$\Delta_f = M_f - M_b \quad (5)$$

3. Results

3.1. Validation of model performance

As precipitation is a source of data for calculating the SPI index, it is crucial to first examine which RCM baseline simulations are able to reproduce observed precipitation. The difference in annual precipitation between the RCM baseline simulations and the observed data is shown in Fig. 3. Overall, simulated models overestimate precipitation from 0 to 300% when compared with the observed data. This result is compatible with those of Nguyen-Ngoc-Bich et al. (2021). All simulated models exhibit an overestimation of about 200% over the Maritime Continent. In the mainland, ECEA and MPI overestimate precipitation by about 200-300%, while CSIRO exhibits a small difference (about 40%) with the observation, except in southern China. Although HadG shows a small difference with the observations over Laos, Thailand, and northern Vietnam, considerable overestimations are observed over southern China, southern Vietnam, and Cambodia. The CNRM and GFDL have a slight overestimation of precipitation in the majority of the mainland, except for considerable overestimation in southern China and Myanmar. In summary, despite large differences between models, the high uncertainty of precipitation is observed over the Maritime Continent, southern China, and Myanmar for all models. The Ens product indicates a better agreement in simulated precipitation with observation among models.

Before analyzing model simulations for drought projections, we test the accuracy of model estimations with observations for the baseline. Drought characteristics, including drought duration, drought severity, inter-arrival time, and maximum intensity of drought, have thus been used for validation. The validation can be used to determine which regions of the Ens data are more or less reliable. The color red means an overestimation of the characteristics. Figure 4 depicts the difference in DD between the model baseline simulations and observations. Overall, the DD differences range from -10 to 5 months for all models. The underestimated DD has been found in many places across the SEA, particularly on the Indonesian island of Borneo and in Myanmar. With the estimation of the Ens, there is a significant underestimation of DD over the Maritime Continent and some areas to the north of the mainland, a slight overestimation of DD over southern Vietnam, and no significant changes in the other areas.

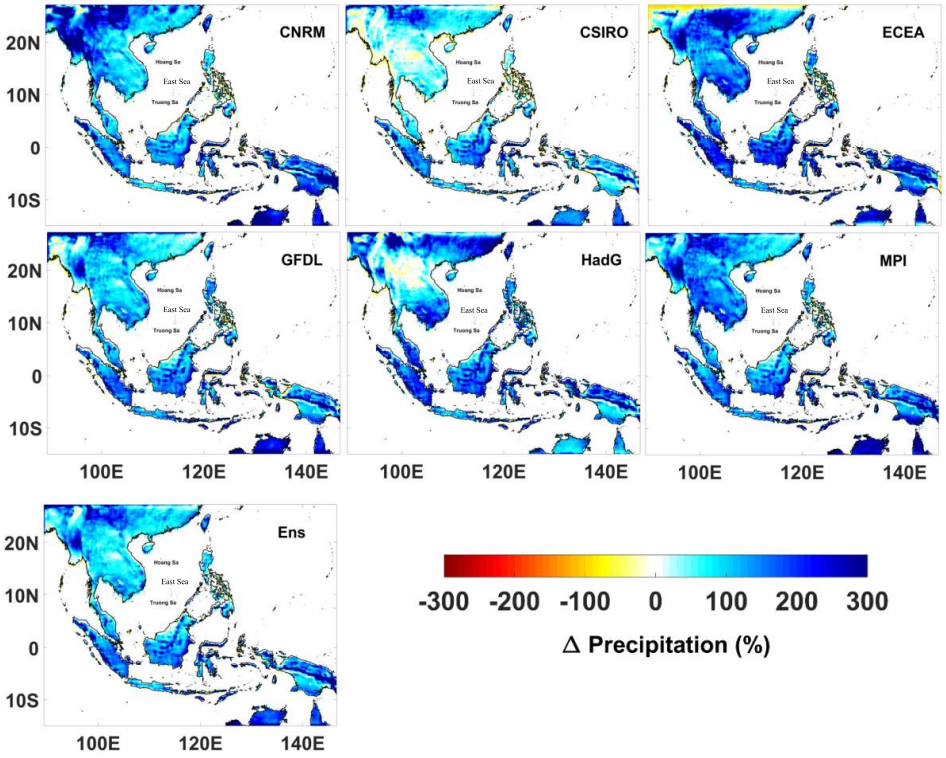

Figure 3. Difference (Δ) in annual precipitation (%) between simulations and observation for the baseline 1976-2005

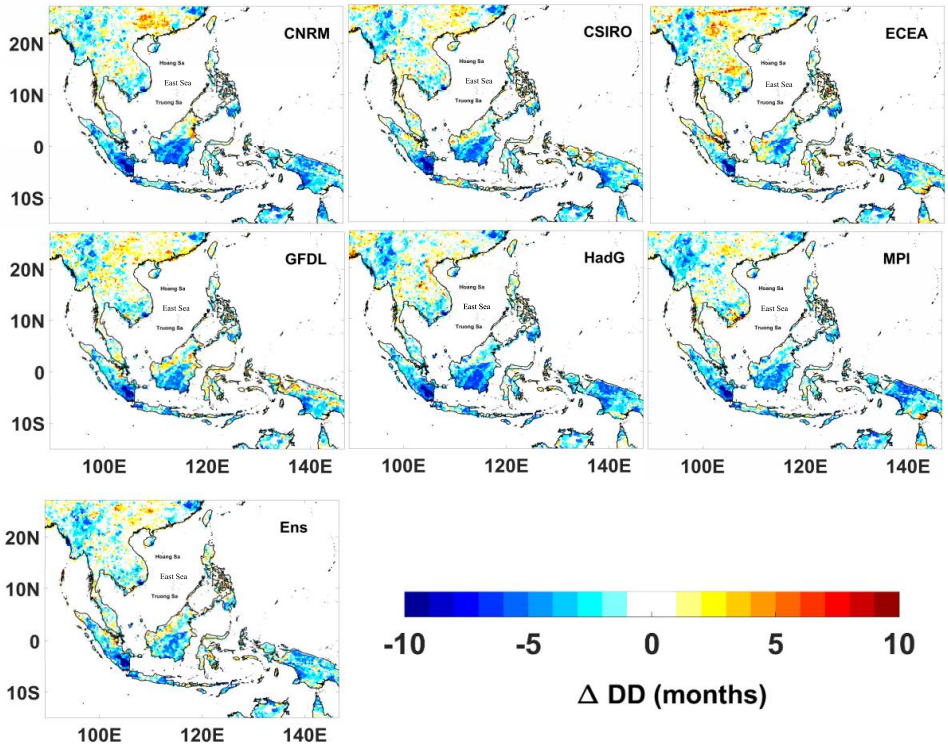

Figure 4. Difference (Δ) in Drought duration (months) between simulations and observation for the baseline 1976-2005

The difference in DS between the baseline simulations and observation data is shown in Fig. 5. In general, all models have underestimations of DS (about 60%) over the majority of the Maritime Continent and Myanmar, and overestimations over some areas in southern China, Laos, Thailand, Malaysia mainland, and the Philippines. ECEA shows the largest overestimation of DS (about 200%) in most of the mainland and some areas of Sumatra islands, Peninsular Malaysia, western Borneo islands and the Philippines. Figure 6 illustrates the difference in ITD between the baseline simulations and observation data. In general, all models have good agreement in presenting patterns of difference in ITD. Remarkable overestimations of about 300% can be observed over east Myanmar, Borneo, Sumatra, and Java islands. The overestimation of ITD indicates that models simulate the period between the beginning of two consecutive droughts longer than observation. These other areas have small differences in the range of -100 to 150%. The difference in averaged maximum intensity of drought between simulated and observed data for the baseline is presented in Fig. 7. Overall, all models underestimate maximum ID (about 50%) in the majority of SEA, particularly in Myanmar, Cambodia, Sumatra, Java, Borneo, and Guinea of Indonesia. Overestimation of maximum ID could be found in some small areas in the mainland and Maritime Continent (i.e., Thailand, southern Vietnam, eastern Sumatra, East Malaysia, the Philippines). Other areas have a small difference in the range of -10 to 10%.

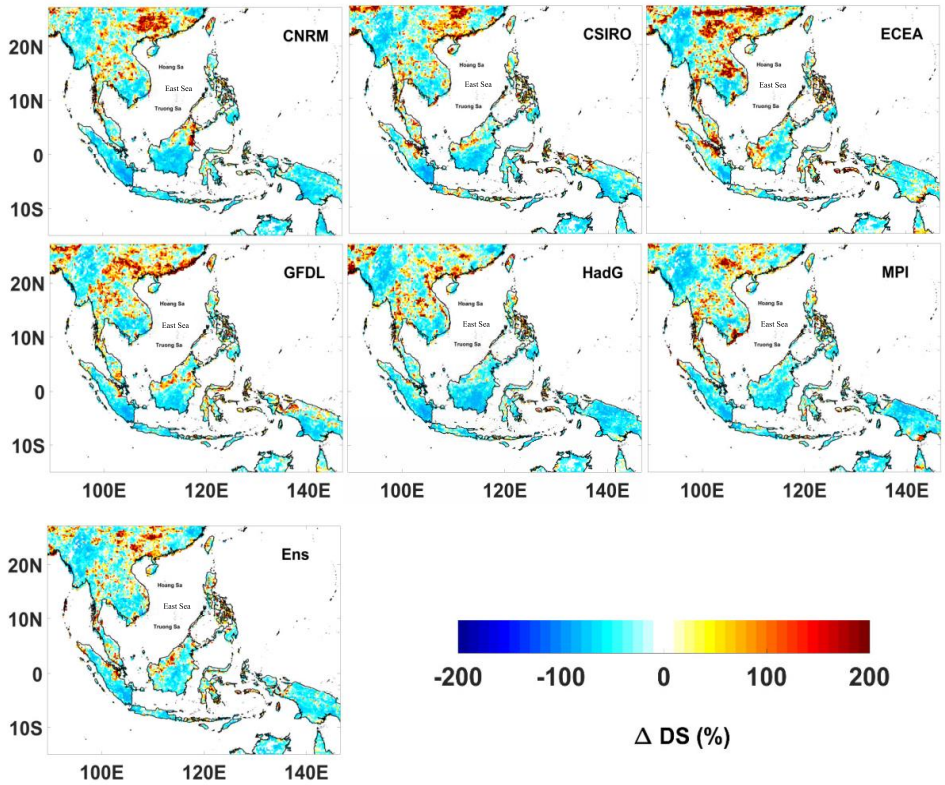

Figure 5. Difference (Δ) in Drought severity (%) between simulations and observation for the baseline 1976-2005

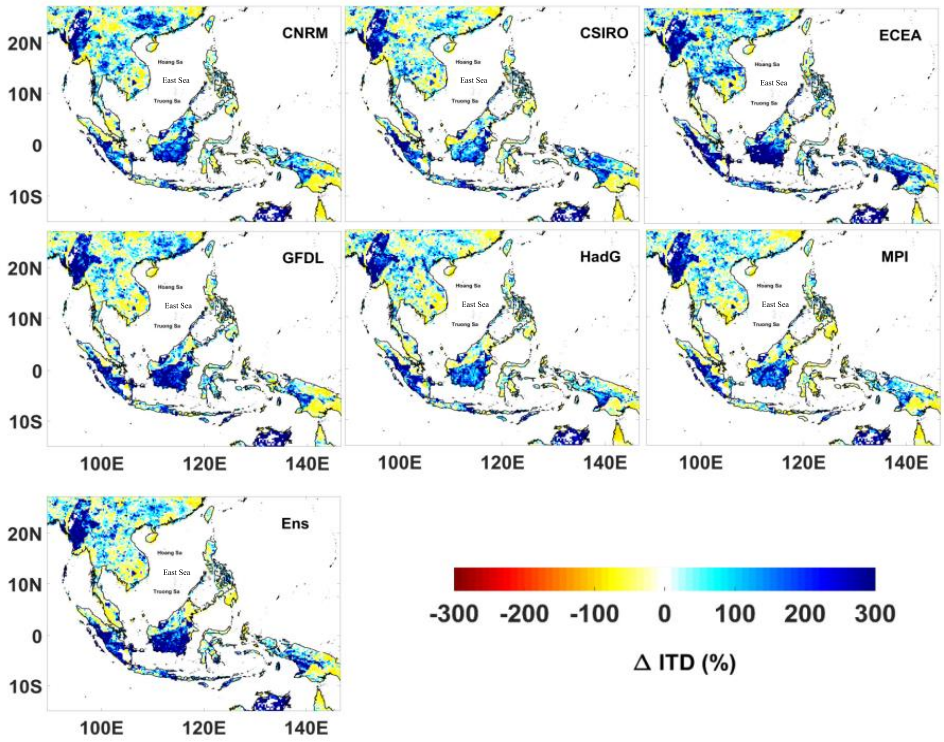

Figure 6. Difference (Δ) in Inter-arrival time (%) between simulations and observation for the baseline 1976-2005

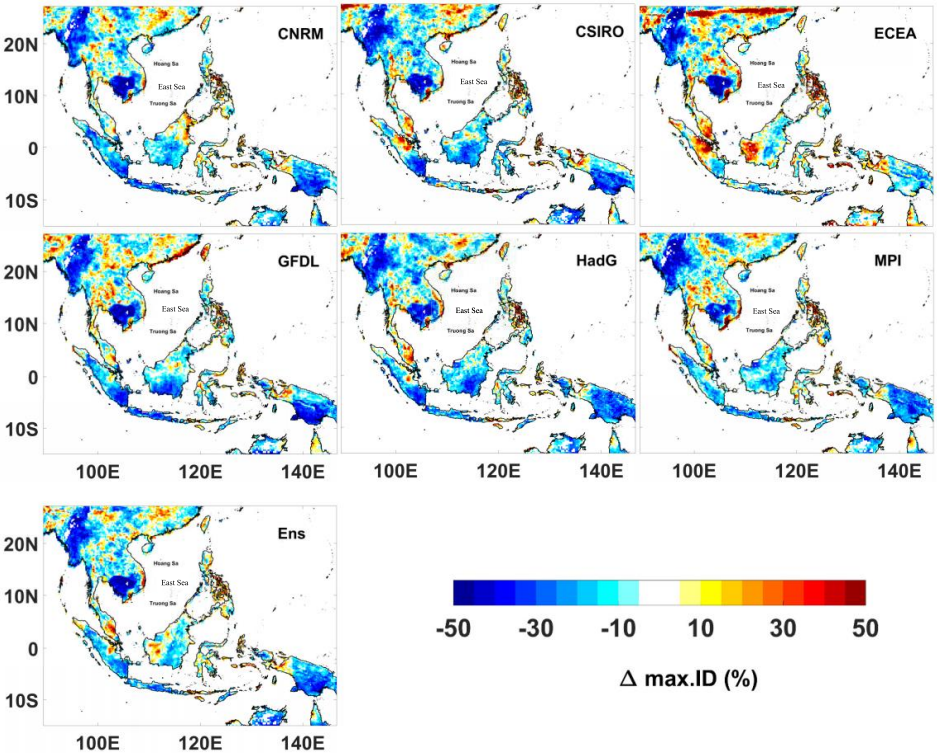

Figure 7. Difference (Δ) in Maximum intensity of drought (%) between simulations and observation for the baseline 1976-2005

In summary, there is a good agreement in simulated precipitation and drought characteristics among models. The Ens model can capture the general features of all models and has the best agreement with observations. As a result, the Ens model was selected to forecast future droughts. The Ens and other models, in general, depict an overestimation of precipitation over SEA. The average duration of drought is shorter than observation in many regions of Indonesia and Myanmar and longer in some small areas of the mainland. Simulated drought severity is less than the observed one in the majority of the region but higher in some areas. Significantly longer inter-arrival time can be found in many regions of Indonesia and Myanmar; and lower maximum intensity can be found in Myanmar, Indonesia, and Cambodia. The overestimation of precipitation may cause an underestimation of drought conditions, particularly over Myanmar and the Maritime Continent.

3.2. Projected changes in annual precipitation and drought characteristics

It is generally agreed that temperatures will increase over the 21st century, so we expect an increase in evapotranspiration and a change in precipitation in the future. To determine where drought becomes more or less severe, we examine the changes in annual precipitation and drought characteristics between future periods (MF and FF) and the baseline under RCP4.5 and RCP8.5.

The projected changes in annual precipitation of the Ens in the MF and FF periods under RCP4.5 and RCP8.5 are shown in Fig. 8. The SEA region is generally projected to decrease in annual precipitation by 0-20%, except for a slight increase in precipitation over southern China and the eastern Guinea Islands. The reduction in precipitation could potentially contribute to the intensity and duration of the drought. In particular, the changes in precipitation in the MF period are not substantial, with slight decreases of 0-5% under RCP4.5 and 0-10% under RCP8.5 over the SEA. In the FF period, there is a greater reduction in precipitation. The large decreases in precipitation are projected at about 15-20% over the majority of SEA under RCP8.5.

Figure 9 depicts the projected changes in DD in the MF or FF periods under RCP4.5 and RCP8.5. Except for some increases in DD observed on the mainland, DD is projected to decrease in most of SEA. In the mid 21st century, large increases in DD are projected mainly in Indochina, while decreases in DD are projected in many areas of the Maritime Continents for both scenarios. In the late 21st century, DD is projected to decrease over SEA for RCP4.5. However, substantial increases in DD are projected over many areas of the mainland with RCP8.5, especially in Thailand.

The projected changes in DS of the Ens model in the MF and FF periods under RCP4.5 and RCP8.5 are presented in Fig. 10. Overall, the changes in DS are in the range of -50 to 200%. Increases in DS are mainly found on the mainland for both RCPs. For the mid 21st century, DS is projected to decrease slightly in the majority of SEA. The considerable increases in DS are projected in some areas of the mainland, Borneo, and Java islands for both climate scenarios. In the late 21st century, remarkable increases in DS occurred mainly on the mainland for RCP8.5, especially over Thailand. There is no significant change in DS over the Maritime Continent for all climate scenarios.

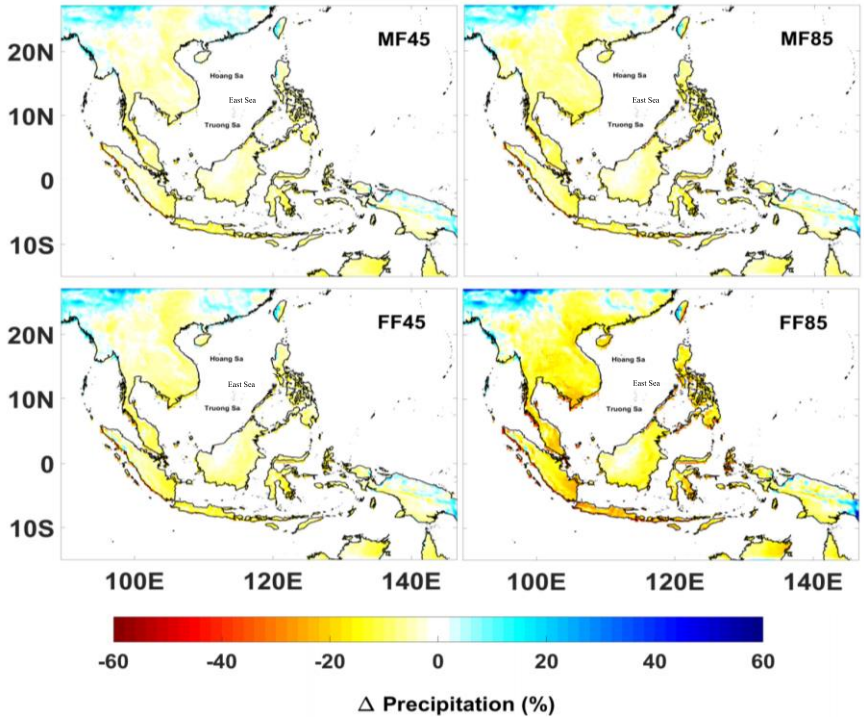

Figure 8. Projected changes in annual precipitation (%) of the Ens in the MF and FF periods under RCP4.5 and RCP8.5

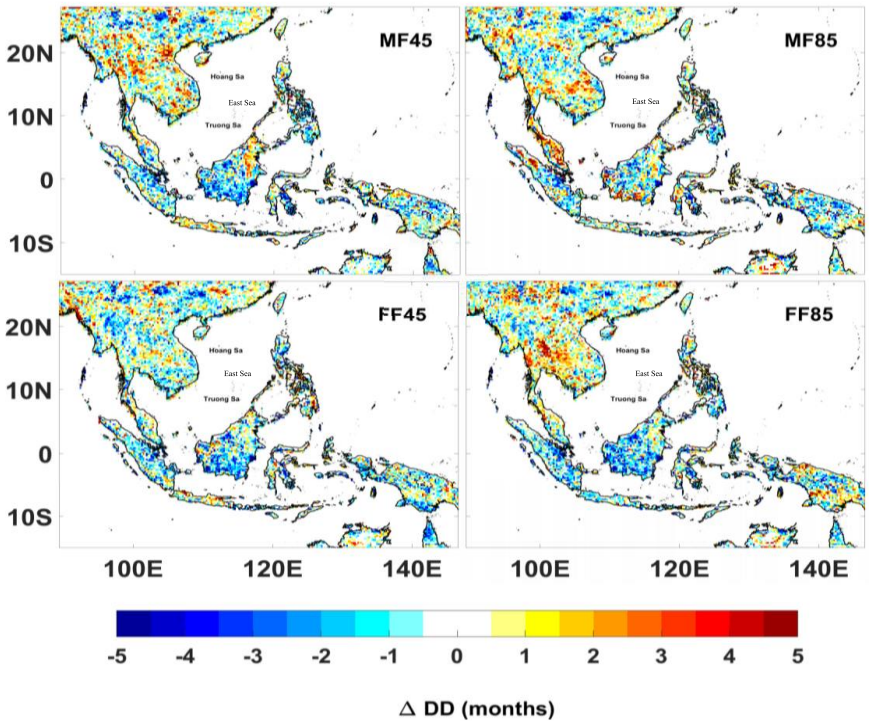

Figure 9. Projected changes in drought duration (DD; month) of the Ens in the MF and FF periods under RCP4.5 and RCP8.5

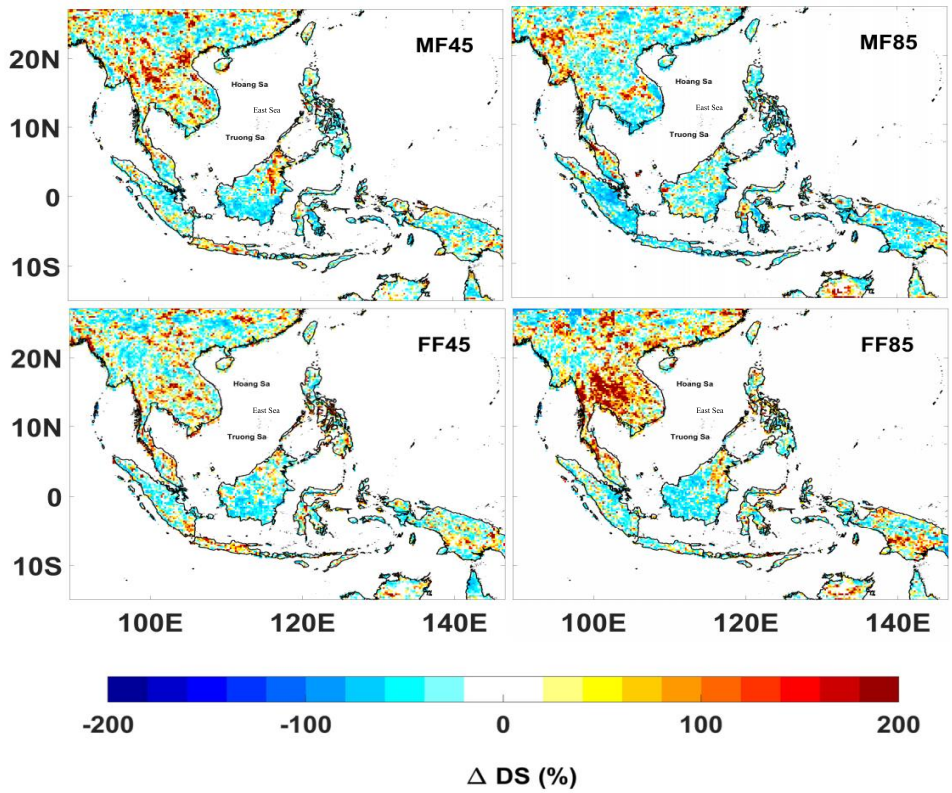

Figure 10. Projected changes in drought severity (DS; %) of the Ens in the MF and FF periods under RCP4.5 and RCP8.5

Projected changes in ITD in the MF and FF periods under RCP4.5 and RCP8.5 are shown in Fig. 11. In general, decreases in ITD are projected for the majority of the SEA for all scenarios, with the exception of some increases over Thailand, northeastern Borneo, northwestern Sumatra, the southern Philippines, and parts of Guinea Island. In the mid-21st century, ITDs are projected to decrease by 60-80%, mainly over Indonesia, southern China, and the northern Philippines. The increase in ITDs is projected mostly in the northeastern part of Borneo and the southern Philippines. In the late 21st century, the decreases in ITDs are mainly observed over the southern Sumatra and Java islands, which are under the equator, under RCP4.5. With RCP8.5, a decrease in ITDs is projected in most of SEA, except for an extensive increase in ITDs over Thailand and apart from Myanmar.

The projected changes in the maximum ID of the Ens in MF and FF periods under RCP4.5 and RCP8.5 are depicted in Fig. 12. In the mid 21st century, maximum ID with RCP45 is projected to change by about 10% over SEA. Maximum ID has decreased substantially throughout SEA with RCP8.5, except in some areas of Myanmar and Borneo island. In the late 21st century, maximum IDs are projected to increase by about 0-30% under RCP4.5 and about 30-60% over the majority of the mainland.

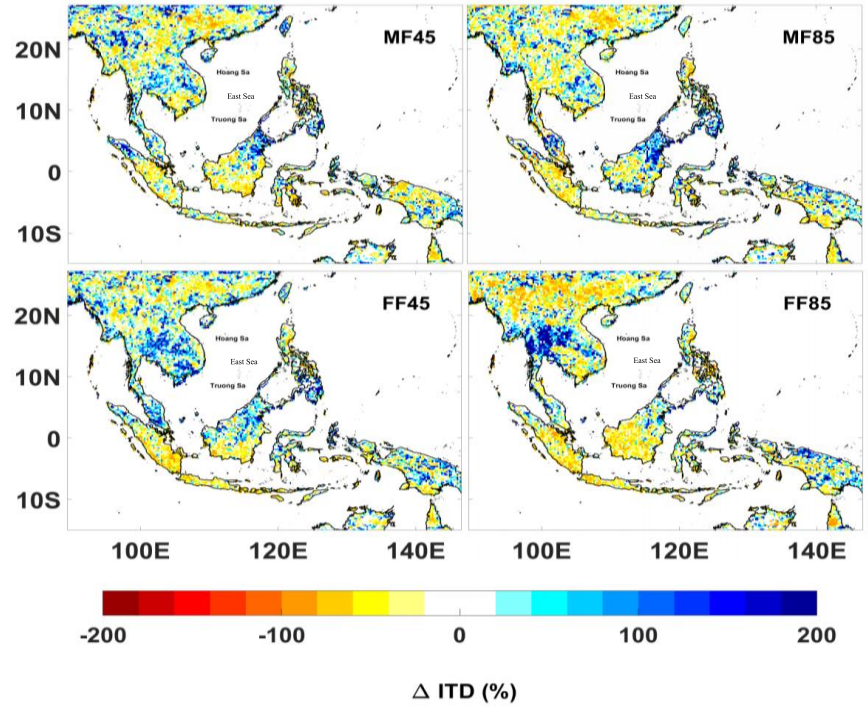

Figure 11. Projected changes in inter-arrival time of drought (ITD; %) of the Ens in the MF and FF periods under RCP4.5 and RCP8.5

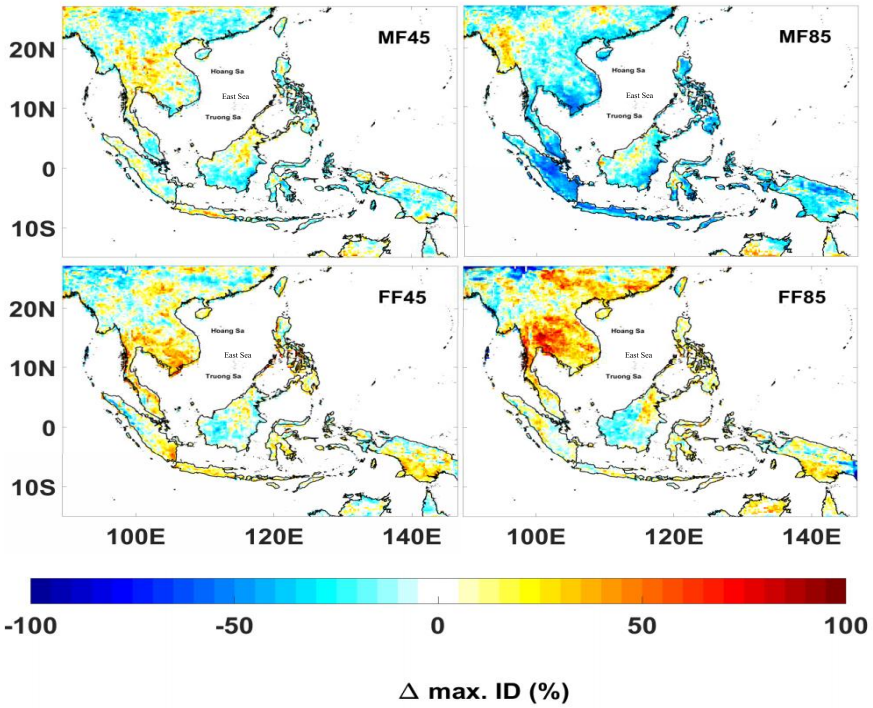

Figure 12. Projected changes in maximum drought intensity (max ID; %) of the Ens in the MF and FF periods under RCP4.5 and RCP8.5

Figure 13 shows projected changes in drought frequency between the future periods and the baseline for SEA under RCP4.5 and RCP8.5. In general, the both scenarios suggest that the changes fluctuate from 0.5 to 3 events per year. The changes in DF fluctuated around 0.5 events per year in the first half of the period, and the amplitude of the fluctuation increased by 0.5 events per year, with the maximum DF change of 3 events per year. The changes with RCP8.5 have the same fluctuation, except for the last two years of the MF period. From 2071 to 2091 in the FF period, the changes fluctuated between 0.2 and 0.8 events per year. DF changes have fluctuated more in the last ten years of the period, ranging from -2 to 3 events/year. The maximum change is an increase of 3 events per year.

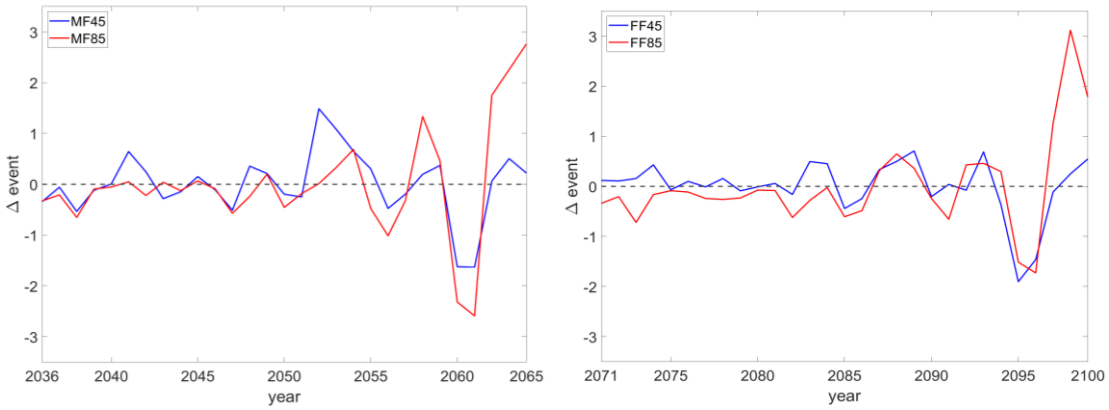

Figure 13. Projected changes in frequency drought (DF, events) of the Ens in the MF (left) and FF (right) periods under RCP4.5 (blue) and RCP8.5 (red)

Figure 14 shows the monthly changes in the spatial geographic extent (%) between the future periods and the baseline under climate scenarios RCP4.5 and RCP8.5. In the mid-century, SE shows little change over the year under both RCP4.5 and RCP8.5. The changes are in a range of -5 to 6%, with the largest change being an increase of 6% in March. At the end of the century, the changes in SE are in a range of -15 to 20% under RCP4.5 and -8 to 10% under RCP8.5. The change in SE based on RCP4.5 seems to be the opposite of the change based on RCP8.5. For example, SE based on RCP4.5 decreases considerably from May to July, whereas there is a little or no change in SE based on RCP8.5 for the same period. In addition, SE based on RCP4.5 increases remarkably from October to December, while SE based on RCP8.5 decreases or shows no change in these months.

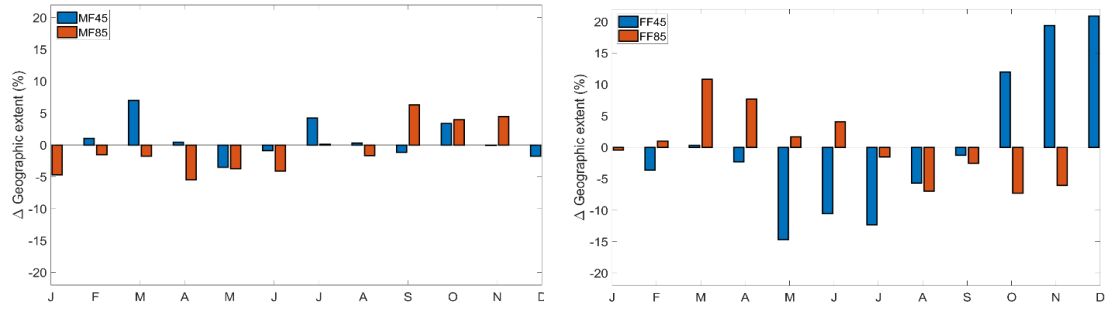

Figure 14. Projected changes in monthly spatial geographic extent (SE, %) of the Ens in the MF (left) and FF (right) periods under RCP4.5 (blue) and RCP8.5 (red)

4. Discussion and Conclusion

This study investigates the projected changes of drought across Southeast Asia in terms of duration, severity, inter-arrival time, maximum intensity, frequency, and geographic extent. The study uses SPI with 12-month time scales based on precipitation data from the multi-model downscaled experiments of CORDEX-SEA. The results show that uncertainty in the individual models is relatively high, and the model ensemble mean (Ens) is the best agreement with observation in simulating precipitation and drought characteristics among models. Therefore, we used the Ens model to examine the future drought characteristics for this study. The choice is consistent with results reported in Raghavan et al. (2018), indicating that no particular model performs well in simulating the observed state of the Southeast Asian climate. In the future, precipitation is projected to slightly decrease over the SEA in the mid-century under both RCP4.5 and RCP8.5, and to remarkably decrease at the end of the 21st century under the RCP8.5 scenario.

Changes in projected drought characteristics based on SPI-12 reveal that drought, in general, is likely to have no significant change by the mid-century. However, worsen drought conditions are expected in some areas of the mainland and the Maritime Continent. At the end of the century, drought conditions are projected to increase significantly in the mainland, with considerable increases in DS and decreases in ITD. The small changes in DD and DS combined with a decrease in ITD over the Maritime Continent demonstrate that the drought events will likely increase over these islands, but they are likely to be shorter and less severe during the late 21st century. Maximum IDs decrease significantly over the SEA by mid-century in both climate scenarios. However, maximum IDs are likely to increase in most of the mainland in the late century under RCP8.5. Frequencies have no significant change (about 0-1 event per year) for the MF and FF periods under both climate scenarios, except for the change of about 3 events per year in the 2060s and 2090s. Monthly geographic extent has no significant change in all months under both scenarios in the mid-century. In the late century, remarkable fluctuations of changes in geographic extent are projected, although there is a disagreement between the changes in geographic extent based on RCP4.5 and the ones based on RCP8.5. Our results agree with the study of Supharatid & Nafung (2021), with shorter drought duration but higher frequency. However, we believe that there will be no or little change in drought conditions in the mid-21st century and that drought conditions will be more severe at the end of the century. Meanwhile, this study suggests that the drought will increase in the near future and decrease in the far future. The uncertainties may arise from the use of data sources (CMIP5 vs. CMIP6) and the choice of drought index. Drought conditions in the Southeast Asian climate are affected by large climate variability due to teleconnections such as the ENSO, the Madden-Julian Oscillation (MJO), and the Indian Ocean Dipole (IOD). Therefore, we suggest examining the changes in climate drivers and their teleconnection with drought conditions to extend the knowledge of drought mechanisms over this region. In addition, we suggest further work to compare the effects of using the SPI and SPEI indices on drought conditions for this region.

Acknowledgments

This research is supported by Vietnam National Foundation for Science and Technology Development (NAFOSTED) under Grant Number 105.06-2019.306. SEACLID/CORDEX-SEA was funded by the Asia-Pacific for Global Change Research (APN) (ARCP2015-04CMY-Tangang, ARCP2014-07CMY-Tangang, ARCP2013-17NMY-Tangang).

References

Abiodun B.J., Makhanya N., Petja B., Abatan A.A.,

Oguntunde P.G., 2019. Future projection of droughts over major river basins in Southern Africa at specific global warming levels. Theoretical and Applied Climatology, 137(3), 1785-1799.

Bayissa Y., Maskey S., Tadesse T., Van Andel S.J., Moges S., Van Griensven A., Solomatine D., 2018. Comparison of the performance of six drought indices in characterizing historical drought for the upper Blue Nile basin, Ethiopia. Geosciences, 8(3), 81.

Brunner M.I., Swain D.L., Gilleland E., Wood A.W., 2021. Increasing importance of temperature as a contributor to the spatial extent of streamflow drought. Environmental Research Letters, 16(2), 024038.

Burke E.J., S.J. Brown, 2008. Evaluating Uncertainties in the Projection of Future Drought. J. Hydrometeorol., 9, 292-299. https://doi.org/10.1175/2007JHM929.1.

Cai W., et al., 2013. Projected response of the Indian Ocean Dipole to greenhouse warming. Nature Geoscience, 6(12), 999-1007.

Cancelliere A., Bonaccorso B., Rossi G., Salas J.D., 2003. On the probabilistic characterization of drought events (Doctoral dissertation, Colorado State University. Libraries).

Cook B.I., J.S. Mankin, K. Marvel, A.P. Williams, J.E. Smerdon, K.J. Anchukaitis, 2020. Twenty-first century drought projections in the CMIP6 forcing scenarios. Earths Future, 8. https://doi.org/10.1029/2019ef001461.

Cook E.R., Seager R., Heim Jr R.R., Vose R.S., Herweijer C., Woodhouse C., 2010. Megadroughts in North America: Placing IPCC projections of hydroclimatic change in a long-term palaeoclimate context. Journal of Quaternary Science, 25(1), 48-61.

Dai A., 2013. Increasing drought under global warming in observations and models. Nat. Clim. Chang., 3, 52-58.

Edwards D.C., 1997. Characteristics of 20th Century drought in the United States at multiple time scales. Air Force Inst of Tech Wright-Patterson Afb Oh.

Emanuel K.A., Živković-Rothman M., 1999. Development and evaluation of a convection scheme for use in climate models. Journal of the Atmospheric Sciences, 56(11), 1766-1782.

Endo N., Matsumoto J., Lwin T., 2009. Trends in precipitation extremes over Southeast Asia. Sola, 5, 168-171.

ESCAP, 2020. Ready for the Dry Years: Building resilience to drought in South-East Asia. United Nations publication.

Giorgi F., Coauthors 2012. RegCM4: model description and preliminary tests over multiple CORDEX domains. Climate Research, 52, 7-29.

Giorgi F., et al., 2009. Addressing climate information needs at the regional level: the CORDEX framework. WMO Bull., 58, 175.

Giorgi F., Huang Y., Nishizawa K., Fu C., 1999. A seasonal cycle simulation over eastern Asia and its sensitivity to radiative transfer and surface processes. Journal of Geophysical Research: Atmospheres, 104(D6), 6403-6423.

Giorgi F., Marinucci M.R., Bates G.T., 1993. Development of a second-generation regional climate model (RegCM2). Part I: Boundary-layer and radiative transfer processes. Monthly Weather Review, 121(10), 2794-2813.

Huo-Po, C., Jian-Qi, S., Xiao-Li, C., 2013. Future changes of drought and flood events in China under a global warming scenario. Atmospheric and Oceanic Science Letters, 6(1), 8-13.

Jamshidi H., Khalili D., Zadeh M.R., Hosseinipour E.Z., 2011. Assessment and comparison of SPI and RDI meteorological drought indices in selected synoptic stations of Iran. In World Environmental and Water Resources Congress 2011. Bearing Knowledge for Sustainability, 1161-1173.

Juneng L., et al., 2016. Sensitivity of Southeast Asia rainfall simulations to cumulus and air-sea flux parameterizations in RegCM4. Climate Research, 69(1), 59-77.

Kim D., Ha K.J., Yeo J.H., 2021. New drought projections over East Asia using evapotranspiration deficits from the CMIP6 warming scenarios. Earth's Future, 9(6), e2020EF001697.

Kim D.-W., H.-R. Byun, 2009: Future pattern of Asian drought under global warming scenario. Theor. Appl. Climatol., 98, 137-150.

Lehner F., S. Coats, T.F. Stocker, A.G. Pendergrass, B.M. Sanderson, C.C. Raible, J.E. Smerdon, 2017. Projected drought risk in 1.5 C and 2 C warmer climates. Geophys. Res. Lett., 44, 7419-7428.

Le H.M., Corzo G., Medina V., Diaz V., Nguyen B.L., Solomatine D.P., 2019. A Comparison of Spatial-Temporal Scale Between Multiscalar Drought Indices in the South Central Region of Vietnam. In Spatiotemporal Analysis of Extreme Hydrological Events. Elsevier, 143-169.

Le-Vu-Viet P., Phan-Van T., Mai-Van K., Tran-Quang D., 2019. Space-time variability of drought over Vietnam. International Journal of Climatology, 39(14), 5437-5451.

McKee T.B., Doesken N.J., Kleist J., 1993. The relationship of drought frequency and duration to time scales. In Proceedings of the 8th Conference on Applied Climatology, 17(22), 179-183.

Mishra A.K., Singh V.P., Desai V.R., 2009. Drought characterization: a probabilistic approach. Stochastic Environmental Research and Risk Assessment, 23(1), 41-55.

Ngo-Duc T., et al., 2017. Performance evaluation of RegCM4 in simulating extreme rainfall and temperature indices over the CORDEX-Southeast Asia region. International Journal of Climatology, 37(3), 1634-1647.

Nguyen-Ngoc-Bich P., et al., 2021. Projected evolution of drought characteristics in Vietnam based on CORDEX-SEA downscaled CMIP5 data. International Journal of Climatology.

Prudhomme C., et al., 2014. Hydrological droughts in the 21st century, hotspots and uncertainties from a global multimodel ensemble experiment. Proc. Natl. Acad. Sci. U.S.A., 111, 3262-3267. https://doi.org/10.1073/pnas.1222473110.

Raghavan S.V., Liu J., Nguyen N.S., Vu M.T., Liong S.Y., 2018. Assessment of CMIP5 historical simulations of rainfall over Southeast Asia. Theoretical and Applied Climatology, 132(3), 989-1002.

Rhee J., J. Cho, 2016. Future changes in drought characteristics: regional analysis for South Korea under CMIP5 projections. J. Hydrometeorol., 17, 437-451.

Rummukainen M., 2010: State-of-the-art with regional climate models. Wiley Interdiscip. Rev. Clim. Change, 1, 82-96. https://doi.org/10.1002/wcc.8.

Seager R., et al., 2007. Model projections of an imminent transition to a more arid climate in southwestern North America. Science, 316, 1181-1184. https://doi.org/10.1126/science.1139601.

Spinoni J., et al., 2020. Future global meteorological drought hot spots: a study based on CORDEX data. J. Clim., 33, 3635-3661.

Spinoni J., G. Naumann, H. Carrao, P. Barbosa, J. Vogt, 2014. World drought frequency, duration, and severity for 1951-2010. Int. J. Climatol., 34, 2792-2804. https://doi.org/10.1002/joc.3875.

Spinoni J., Vogt J.V., Naumann G., Barbosa P., Dosio A., 2018. Will drought events become more frequent and severe in Europe?. International Journal of Climatology, 38(4), 1718-1736.

Supharatid S., Nafung J., 2021. Projected drought conditions by CMIP6 multimodel ensemble over Southeast Asia. Journal of Water and Climate Change, 12(7), 3330-3354.

Sushama L., Said S.B., Khaliq M.N., Kumar D.N., Laprise R., 2014. Dry spell characteristics over India based on IMD and APHRODITE datasets. Climate Dynamics, 43(12), 3419-3437.

Svoboda M., Hayes M., Wood D.A., 2012. Standardized precipitation index user guide. World Meteorological Organization, 1090.

Swain S., Hayhoe K., 2015. CMIP5 projected changes in spring and summer drought and wet conditions over North America. Climate Dynamics, 44(9), 2737-2750.

Tangang F., Farzanmanesh R., Mirzaei A., Salimun E., Jamaluddin A.F., Juneng L., 2017. Characteristics of precipitation extremes in Malaysia associated with El Niño and La Niña events. International Journal of Climatology, 37, 696-716.

Tangang F., et al., 2020a. Projected future changes in rainfall in Southeast Asia based on CORDEX--SEA multi-model simulations. Clim. Dyn., 55, 1247-1267.

Tangang F., et al., 2020b. Multi-model projections of precipitation extremes in Southeast Asia based on CORDEX-Southeast Asia simulations. Environmental research, 184, 109350.

Thilakarathne M., V. Sridhar, 2017. Characterization of future drought conditions in the Lower Mekong River Basin. Weather and Climate Extremes, 17, 47-58.

Touma D., M. Ashfaq, M.A. Nayak, S.-C. Kao, N.S. Diffenbaugh, 2015. A multi-model and multi-index evaluation of drought characteristics in the 21st century. J. Hydrol., 526, 196-207.

van Vuuren D.P., et al., 2011. The representative concentration pathways: an overview. Climatic Change, 109, 5-31.

Yatagai A., Kamiguchi K., Arakawa O., Hamada A., Yasutomi N., Kitoh A., 2012. Aphrodite: Constructing a long-term daily gridded precipitation dataset for Asia based on a dense network of rain gauges. Bulletin of the American Meteorological Society, 93(9), 1401-1415.

Zhai J., et al., 2020. Future drought characteristics through a multi-model ensemble from CMIP6 over South Asia. Atmos. Res., 246, 105111.

Zhang L., T. Zhou, 2015. Drought over East Asia: a review. J. Clim., 28, 3375-3399.

Zhao T., A. Dai, 2017. Uncertainties in historical changes and future projections of drought. Part II: model-simulated historical and future drought changes. Clim. Change, 144, 535-548.